B_1 gradient encoding with the rotating RF coil

Adnan Trakic[1], Ewald Weber[1], Ming Yan Li[1], Jin Jin[1], Feng Liu[1], and Stuart Crozier[1]
[1]*The School of ITEE, The University of Queensland, Brisbane, QLD, Australia*

Synopsis: Conventionally, magnetic resonance imaging (MRI) is performed by pulsing gradient coils, which invariably leads to strong acoustic noise, eddy current induction in nearby conductors/patient, and costly power and space requirements. Here we describe a new silent, B_0 gradient-free MRI technique, B_1 gradient encoding with a rotating RF coil (B_1-RRFC). The rotation of the RF coil allows for the generation of a large number of B_1 gradients over time. Coupled with a flip angle – based modulation scheme as part of a finite-difference-based nonlinear Bloch equation solver, the RRFC technique facilitates a large number of encoding degrees of freedom. Initial results suggest that representative 2D and 3D images with intensity deviations of less than 5% from the original image can be obtained.

Methods: In recent studies we have demonstrated that mechanically rotating a single RF transceive coil (RRFC) can imitate a large RF coil array by time-division-multiplexing (TDM) [1-2]. In this new study, we show that the RRFC transmit concept can be applied to B_1 gradient encoding using nonlinear RF gradients. For each encoding step, a single data point is measured during the free induction decay, filling the 3-dimensional (3D) *pseudo k-space D* [3]:

$$D_{\theta,\alpha,\beta} \sim \int \vec{M}(\vec{r})\frac{\vec{B}_{1\theta}(\vec{r})}{\left|\vec{B}_{1\theta}(\vec{r})\right|}\sin\left(\gamma\tau g_\alpha g_\beta \Delta\left|\vec{B}_{1\theta}(\vec{r})\right|\right)dV \quad (1)$$

$$E_{j,(\theta,\alpha,\beta)} = \frac{\vec{B}_{1\theta}(\vec{r}_j)}{\left|\vec{B}_{1\theta}(\vec{r}_j)\right|}\sin\left(\gamma\tau g_\alpha g_\beta \Delta\left|\vec{B}_{1\theta}(\vec{r}_j)\right|\right) \quad (2)$$

$$\vec{M}^{n+1} = \gamma\vec{M}^n + \frac{\gamma\Delta t}{1+\frac{1}{4}\Delta t^2 B^2}\left(\vec{M}^n + \frac{1}{2}\Delta t\,\vec{M}^n \times \vec{B}\right)\times\vec{B} \quad (3)$$

where $D_{\theta,\alpha,\beta}$ is the measurement, $\vec{M}(\vec{r})$ is the signal intensity, γ is the gyromagnetic ratio, τ is the RF pulse duration, $\vec{B}_{1\theta}(\vec{r})$ is the complex RF magnetic field (gradient) at coil position $\theta(t) = \omega_{rot}t$ (where ω_{rot} is the angular frequency of RF coil rotation), g_α and g_β are the α^{th} and β^{th} B_1-gradient scaling factors, which are a function of time (and part of the imaging sequence). Image reconstruction from k-space is performed via matrix inversion of Eq.(1): $D = EG$ (4), with D a vector containing $I = \theta\alpha\beta$ complex data points, G containing the values of magnetization $\vec{M}(\vec{r})$ discretised on a spatial grid of $J = NML$ voxels, and E the J x I encoding matrix Eq.(2), where (N,M,L) and (θ,α,β) are the discrete dimensions of the MR image and k-space, respectively. The desired distribution $\vec{M}(\vec{r})$ can be reconstructed by solving of Eq.(4) via $G = E^{+}D$, where image $\vec{M}(\vec{r})$ is obtained by restricting the 1-dimensional vector G to a 3-dimensional matrix. An unconditionally stable finite-difference based solution of Bloch Eq. (3) [4] is used with Eq. (4) to simulate the nonlinear behaviour of the spin system.

Results and discussion: The B_1^+ field map of the rotating RF coil (Fig.1) was obtained by dividing the image by a uniform reference followed by a series of post-processing operations involving: thresholding, polynomial fitting and phase unwrapping. To generate the pseudo k-space data, we rotated the sensitivity map at $\omega_{rot} = 90\ rad\ s^{-1}$ and applied a gauss RF pulse of τ = 5ms in duration. The experiment was repeated M = 100 number of times, wherein the strength of the pulse was incremented with each phase encoding step according to $g_\alpha = \alpha - M/2 - 1/2,\ g_\beta = 1$. The RF pulse power was adjusted to generate a maximum 90° flip angle when α = 100. Matrix E was then populated according to Eq.(2) by rotating the B_1^+ map via complex plane rotation and spline interpolation routines. System Eq. (4) was solved using Bloch adapted - least square QR factorisation method with initial magnetization conditions of: $M_x = 0$, $M_y = 0$ and $M_z = 1A/m$. For every incremental map rotation, $\pm 0.2\%$ random noise was added to simulate noise propagation. Similarly, B_1-RRFC can be applied without any B_0-gradients by varying the amplitude of the B_1 pulse along the two (D_α, D_β) of the three k-space dimensions, i.e. according to: $g_\alpha = \alpha - M/2 - 1/2$ and $g_\beta = \beta - L/2 - 1/2$.

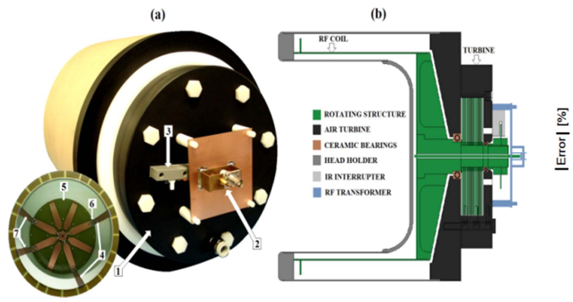

Fig.1 – (a) Photograph and (b) side view of the rotating RF coil (RRFC) system consisting of (1) air turbine, (2) the inductively coupled RF link, (3) infra-red photo-interrupter, (4) RF coil, (5) PCB and (6) tuning capacitor.

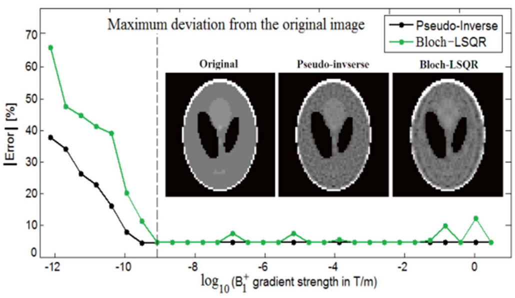

Fig.2 – B_1-RRFC of the Pseudo-inverse and Bloch-LSQR method versus the unit B_1^+-gradient (NxM=64x64). The system converges to <5% when the unit B_1-gradient is at least 10^{-9} T/m.

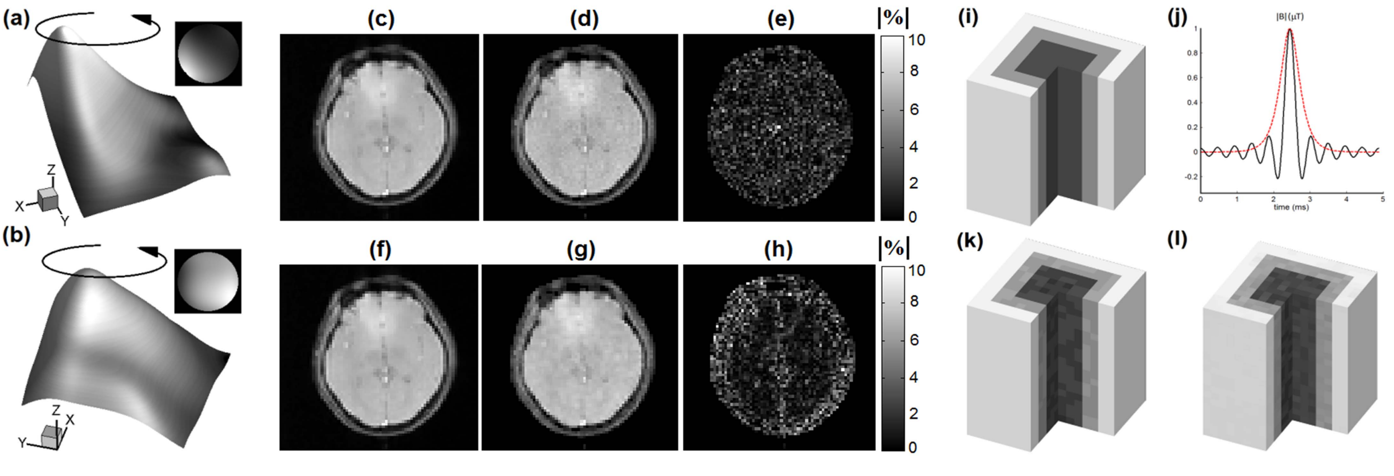

Fig.3 – Surface plots of polynomial-fitted, spatially nonlinear 2D B_1^+ gradient field obtained with the FLASH imaging sequence: (a) magnitude and (b) unwrapped phase based on the data obtained with the RRRC system in Fig.1. Comparison of B_1-RRFC image reconstruction results (N x M = 100 x 100) including the: (c) and (f) (normalized) original, (d) pseudo-inverse and (g) Bloch-LSQR; as well as the absolute value deviation maps (from the original image) in |%|: (e) pseudo-inverse and (h) Bloch-LSQR. To solve Eq.(4) using the Bloch-LSQR approach it took around 21.2min and 4.77GB of RAM. 3D-B_1-RRFC encoded results using Bloch-LSQR solver: (i) original image (21x21x21 voxels), (j) normalized *sinc* (line) and *sech* (dotted line) RF pulses (absolute magnetic flux density in μT over time), (k) 3D-B_1-RRFC using *sinc* and (l) 3D-B_1-RRFC using *sech* RF pulse (with $\omega_{rot} = 628\ rad\ s^{-1}$).

According to Fig.2, the deviation from the original image intensity converges to about 4.92% for unit B_1 gradients larger than about 1nT/m, which are easily achieved in practice. From Fig.3 (e-h), the maximum percentage deviation of the pseudo-inverse and Bloch-LSQR reconstructed images from the magnitude normalized original image were 9.2% and 8.7%, respectively. While 2-dimensional examples employed the z-gradient coil only to select the slice of magnetization, Fig.3 (i-l) shows the results of B_1-RRFC encoding with 3D B_1 gradients using two different RF pulses (*sinc* and *sech*) without the application of any B_0 gradients.

Conclusion: A new B_0 gradient-free B_1-RRFC method was described. The rotation of the RF coil provides a significant number of B_1 gradients over time which can facilitate complex modulation of magnetization. The results obtained suggest that representative MR images can be obtained using the B_1-RRFC concept. Potential applications of this concept include silent, low-cost and simplified (gradient coil - free) MRI equipment.

References:
A. Trakic et. al. JMR 201(2), 2009.
A. Trakic et. al. IEEE Trans. Bio. Eng. 59(4), 2012.
U. Katscher et. al. MRM 15, 2007.
M. Olko et. al. Physica, 176, 1991.